Pre-Mesozoic interpreted bedrock geology of the southwest Yilgarn, 2021

by

R Quentin de Gromard, TJ Ivanic and I Zibra

Abstract

Introduction

The pre-Mesozoic interpreted bedrock geology map of the southwest Yilgarn (Fig. 1; Geological Survey of Western Australia [GSWA], 2021) integrates legacy data with a substantial volume of new data from multiple datasets acquired under the Accelerated Geoscience Program (AGP). The objective of this interpreted bedrock geology map is to achieve a uniform interpretation of the geology across the southwest of the Yilgarn Craton (south–central part of the South West Terrane of Cassidy et al., 2006). It provides context for known mineral deposits in the region and aims to open new search space in this underexplored and highly prospective portion of the Yilgarn Craton.

This extended abstract is intended to be used in conjunction with the interpreted bedrock geology digital layers and with the other ~600 digital layers provided within the Southwest Yilgarn, 2021 Geological Exploration Package (GSWA, 2021).

The southwest Yilgarn interpreted bedrock geology map area is approximately 450 x 380 km wide and is bounded in the west by the Darling Fault, and in the east by the Southern Cross – Forrestania – Ravensthorpe greenstone belts. It includes the Wongan Hills and Westonia greenstone belts in the north and extends into the Albany–Fraser Orogen in the south. The area encompasses the informal Balingup, Boddington and Lake Grace terranes of Wilde et al. (1996). One of the most significant outcomes of our interpretation is a change in the subdivision of Yilgarn Craton terranes. The nomenclature of Wilde et al. (1996) is not fully adopted here because our interpretation shows that the Lake Grace terrane represents a higher metamorphic grade equivalent to the Youanmi Terrane. The extent of our redefined South West Terrane is nearly identical to the extent of the combined Boddington and Balingup terranes of Wilde et al. (1996). No attempt has been made to subdivide the redefined South West Terrane due to insufficient age data. The Proterozoic Cardup Basin has not been included in this version of the southwest Yilgarn interpreted bedrock geology but may be added in a future iteration of this map.

The interpreted bedrock geology map consists of five interpretative layers:

- ‘Terrane boundary’ layer, which consists of the trace of the interpreted terrane boundary between the Youanmi and the South West Terranes based on tracing existing structure lines from the ‘structure line’ layer below.
- ‘Geophysical line’ layer, which consists of lines interpreted from aeromagnetic data. These are to be regarded as form lines and represent the aeromagnetic signature of primary fabrics including bedding and magmatic layering, or secondary fabrics such as tectonic foliation, gneissic layering or attenuated and dismembered layers forming boudin trains.
- ‘Geological line’ layer, which primarily comprises the trace of mafic dykes but also of narrow geological units that are too thin to be represented as polygons, such as felsic dykes and banded iron-formations (BIF).
- ‘Structural line’ layer, which contains faults and shear zones and includes attributes, where known, such as dip estimate, dip direction, kinematic information and inferred maximum and minimum ages.
- ‘Geological polygon’ layer containing the geologically coded map units and, where known, unit names, descriptions and geochemical classification of granites.

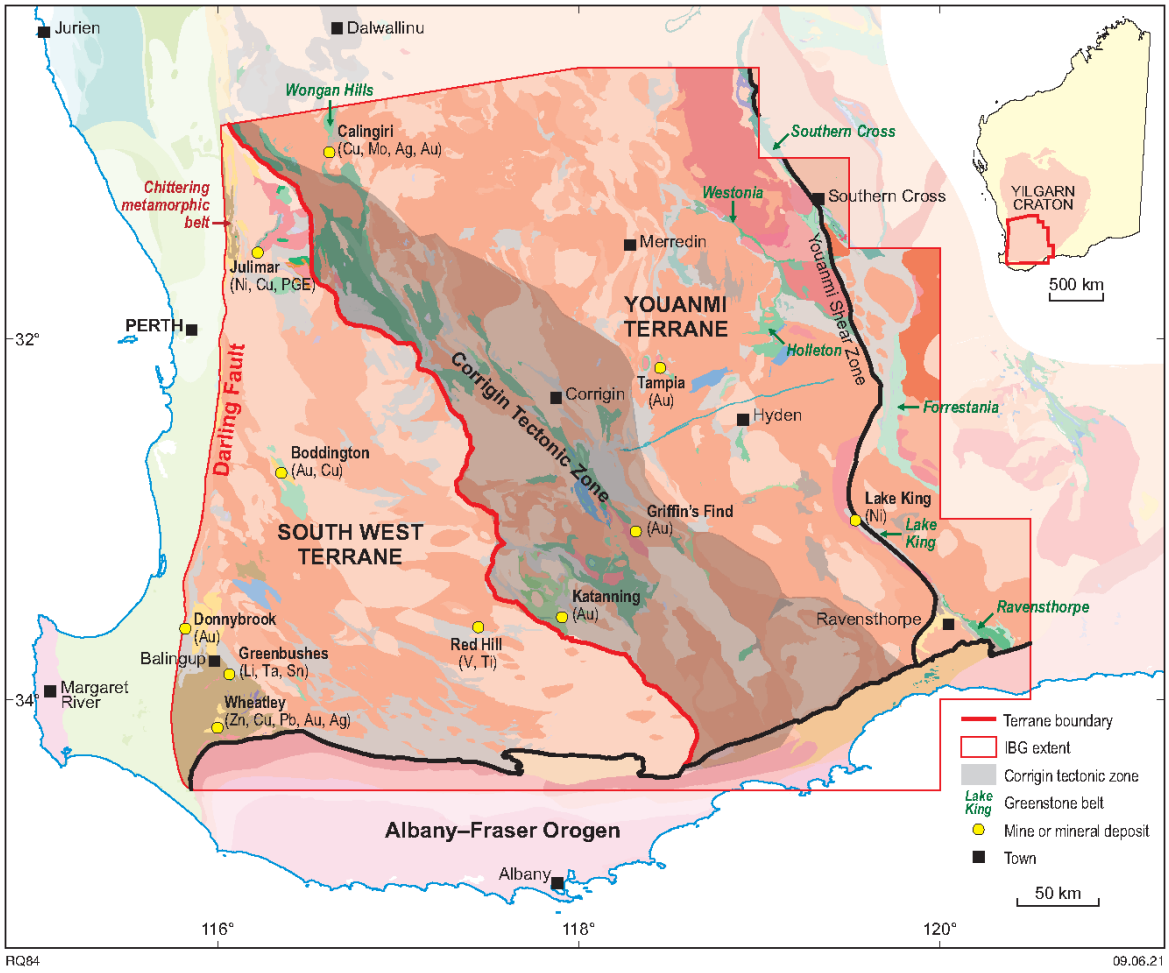

Figure 1. Simplified pre-Mesozoic interpreted bedrock geology (IBG) of the southwest Yilgarn, showing the new mapping produced during the southwest Yilgarn project of the AGP, overlying the 1:500 000-scale state IBG polygon layer. The thick red line shows the location of the redefined terrane boundary between the Youanmi and South West Terranes, the yellow dots show the location of the main mines and mineral deposits west of Youanmi Shear Zone; the main commodities are shown in brackets. To view all layers of the southwest interpreted bedrock geology, see the Southwest Yilgarn, 2021 Geological Exploration Package (GSWA, 2021)

Data

A vast number of features contained within various legacy and AGP datasets and publications have contributed to the making of this interpreted bedrock geology map and are included, where possible, as digital layers on the Southwest Yilgarn, 2021 Geological Exploration Package (GSWA, 2021). These supporting layers include:

- GSWA field observations captured in WAROX (GSWA, 2020a)
- GSWA digital WAROX text searches layer (Ivanic et al., 2021a)
- GSWA digital granite geochemical classification layer (Smithies et al., 2021a)
- GSWA digital greenstone geochemistry layers (Ivanic et al., 2021b)
- GSWA U–Pb zircon geochronology (GSWA, 2020b)
- GSWA Sm–Nd and zircon O isotope maps of Western Australia (Lu et al., 2021a,b)
- GSWA MINEDEX Mines and Mineral deposits layers
- GSWA Metamorphic History records of the southwest Yilgarn (Korhonen et al., 2021)
- legacy GSWA 1: 250 000 surface geology and explanatory notes (including their 1: 250 000 interpreted geology figures)

- existing GSWA interpreted bedrock geology digital layers at 1:100 000 and 1: 500 000 scale
- numerous, georeferenced company maps (GSWA, 2021)
- new, detailed field mapping of the Chittering Metamorphic Belt (at approximately 1:50 000 scale) conducted and compiled by Zibra (2021) was seamlessly incorporated into the southwest Yilgarn interpreted bedrock geology
- aeromagnetic compilation images including multi-scale edges (Brett, 2021; GSWA, 2021). The line spacing of individual available (open file and confidential) surveys ranges from 25 to 400 m over the whole interpreted bedrock geology map area, with over two-thirds of the map area covered by 100 m line spacing or less. The aeromagnetic compilation images employed a 40 x 40 m cell size, optimized for 150 m, or greater, line spacing. Where available, high-resolution surveys were used to obtain the highest confidence level in interpretation of specific areas
- open file gravity data including multi-scale edges (Brett, 2021; GSWA, 2021)
- external publications and theses.

Methods and interpretation

Two field trips were conducted at the start of the project to provide spatial and geological context for all existing data, and in particular, to develop an understanding of deformation style, strain intensity, metamorphic grade and main lithostratigraphic units, and to provide regional context to known mineral deposits.

Over the whole interpreted bedrock geology map area, the uniformity of the data structure and the relatively high density of the individual point datasets has allowed for consistency of geological interpretations during map compilation with a high level of confidence. The geological point datasets were systemically correlated with the gravity and aeromagnetic compilation images (Brett, 2021; GSWA, 2021). The potential field data compilation images, being derived from multiple datasets of different resolution, enabled consistency of interpretation across the whole map area. Correlating mappable polygons from the aeromagnetic dataset from point data was achieved primarily in areas of high point data density, and then extrapolated into the areas of lesser data density. Geological interpretation and a matrix of relative event timing were progressively built during the map compilation process. We systematically recorded crosscutting relationships between the various geological features with the same principles used during field mapping. The compilation over most of the interpreted bedrock geology extent was constructed at between 1:40 000 and 1:65 000 scale and is intended to be best viewed at 1:250 000 scale.

The primary focus was on the central part of the map area, whereas the southern and eastern edges were left practically unchanged from existing 1:100 000 and 1:500 000 mapping; the latter mapping is included in the southwest Yilgarn interpreted bedrock geology for edge matching purposes. For example, the eastern part of the SOUTHERN CROSS 1:100 000 map sheet as well as the Forrestania and Ravensthorpe greenstone belts from GSWA 1:500 000 digital layers were imported from the existing digital compilation and blended into the southwest Yilgarn interpreted bedrock geology.

In the following paragraphs we will describe the layers as they are displayed in the Southwest Yilgarn, 2021 Geological Exploration Package.

Geolines

5922 line segments were interpreted and digitized into the geoline layer ('Interpreted pre-Mesozoic bedrock geology lines, 2021') of the interpreted bedrock geology. This layer largely consists of interpreted mafic dyke segments assigned to 12 different dyke suites or members of such suite (Fig. 2). The mafic dyke compilation is largely based on a previously published statewide dyke layer (Wingate, 2017) on an unpublished compilation (T. Beardsmore, written communication, 2020), and on recently dated dykes (Stark et al., 2018a,b; Stark et al., 2019). Each line segment is attributed with a code, a unit name, a description and, where available, with an age and a magnetic polarization (either positive or negative). The mafic dykes were entirely (re-)drawn from the high-resolution aeromagnetic dataset, to ensure that crosscutting relationships between dykes and structures were systemically captured and interpreted consistently. The main aeromagnetic images used were the 'TMI_RTP_drape90_colour', the 'TMI_RTP_1VD_colour' and the 'TMI_RTP_1VD_grey' images. Additionally, the 'TMI_AnS_drape' image was used to avoid misinterpreting a negatively magnetized mafic dyke for a demagnetized fault and vice versa. Minor geolines, other than mafic dykes, such as BIF, chert, felsic dykes, pegmatite or quartz veins were are also included in this layer, and mostly in the marginal parts of the southwest Yilgarn interpreted bedrock geology map area.

Twelve mafic dyke suites or members of such suites were identified and digitized (Fig. 2). In relative chronological order, these are:

- A north- to northeast-trending, Archean mafic dyke suite, interpreted to be c. 2640 Ma in age, is here informally named the 'Babakin metadolerite'. This undated suite was identified from aeromagnetic data primarily within the Corrigin Tectonic Zone and is interpreted as a suite of deformed mafic dykes emplaced synchronously with the syn- to post-tectonic intrusions of the c. 2651–2630 Ma low-Ca, P-rich granites. These dykes all have a positive magnetic polarity.
- c. 2615 Ma northeasterly to north-northeasterly trending Yandinilling Dolerite, dated by Stark et al. (2018a). These dykes are largely restricted to the northwest portion of the map area. They crosscut and are not affected by the Corrigin Tectonic Zone and thus form an absolute minimum age for this deformation event. Most of these dykes are 'positive', but few negatively polarized dykes occur.
- c. 2410 Ma westerly to west-southwesterly trending Widgiemooltha Dolerite. Individual dyke segments are commonly 100–200 km long, and occur over most the map area. This dyke swarm hosts some of the widest mafic dykes in the map area, which are locally up to ~600 m wide. Both positive and negative magnetic polarities occur and the age of this magnetic pole reversal was previously bracketed between 2408 ± 3 Ma and 2401 ± 2 Ma for a 'positive' and a 'negative' dyke, respectively (Wingate, 2007; Pisarevsky et al., 2015).
- c. 1888 Ma west-northwesterly trending Boonadgin Dolerite dated by Stark et al. (2019). These dykes mostly occur in the southwest portion of the map area and are almost entirely restricted to the redefined extent of the South West Terrane. These dykes all preserve a positive magnetic polarity.
- c. 1390 Ma north-northwesterly trending Biberkine Dolerite, dated by Stark et al. (2018b). The dykes occur in the western part of the map, and were mostly intruded into the redefined extent of the South West Terrane, but also within the southwestern margin of the Youanmi Terrane. These dykes are emplaced along and parallel to the terrane boundary, and lie parallel to the regional to terrane-scale, north-northwesterly trending, long-wavelength gravity anomaly that underlies the South West Terrane. Both 'positive' and 'negative' dykes occur.

- Dykes of the c. 1210 Ma Marnda Moon Large Igneous Province:
    - The northwesterly trending Boyagin Dolerite. These dykes also largely occur in the redefined extent of the South West Terrane; only minor occurrences were interpreted east of the terrane boundary. These dykes all preserve a positive magnetic polarity.

  - The west-southwesterly trending Gnowangerup–Fraser Dolerite, occurring in the southern portion of the map area, across the Youanmi and South West Terranes, and emplaced parallel to the western Albany–Fraser Orogen margin. Both 'positive' and 'negative' dykes occur.
  - The west-northwesterly trending Wheatbelt Dolerite. These dykes occur in the northern portion of the map area and were mostly intruded into the Youanmi Terrane. These dykes all preserve a positive magnetic polarity.
- The undated northwesterly trending Beenong Dolerite, bracketed between c. 1218 and 541 Ma, occurring in the eastern part of the map area and exclusively within the Youanmi Terrane. These dykes mostly preserve a positive magnetic polarity, only minor 'negative' dykes were identified.
- Undifferentiated Proterozoic mafic dykes mostly occurring in the far southwestern corner of the map are abundant and tightly spaced, all preserving a positive magnetic polarity.
- c. 733 Ma west-northwesterly trending Nindibillup Dolerite, rare and limited to the redefined extent of the Youanmi Terrane, these dykes can be hundreds of kilometres long and preserve both positive and negative magnetic polarity.

Form lines

A total of 7864 form lines interpreted from aeromagnetic data were interpreted and digitized into the geophysics layer (geophys_lne) of the interpreted bedrock geology map. Entirely interpreted from aeromagnetic data, these lines represent the aeromagnetic signature of primary fabrics such as bedding or magmatic foliation or secondary fabrics such as tectonic foliation, folds or boudin trains. This layer should be regarded as a form line interpretation and be primarily used as a representation of the ductile architecture of the crust subsurface. The form lines are particularly useful to estimate strain intensity, to map shear zones by localizing truncations and attenuation of various markers, and interpret the kinematics of faults and shear zones from offsets and drag of primary or secondary layering. Thus, map domains with different geometries of form lines can potentially suggest that these domains experienced differing geological histories.

Structural lines

To understand the structural framework, initially a first-pass, interpreted bedrock geology-wide, structural framework of main shear zones and faults was established. Large-scale faults and shear zones were mostly interpreted using Bouguer gravity (SWYC_grav_drape_), isostatic residual gravity (SWYC_graviso_drape_) and multi-scale edges (Brett, 2021; GSWA, 2021) together with upward continued (Up) images of the reduced to pole (RTP), total magnetic intensity (TMI) data with upward continuation values of 10 km, 1 km and 500 m (SWYC_tmi_RTPUp10km, SWYC_tmi_RTPUp1km, SWYC_tmi_RTPUp500m) variously coloured or as greyscale images as well as the magnetic integral images ('pseudogravity', SWYC_tmi_RTPInt_drape) and magnetic multi-scale edges (Brett, 2021; GSWA, 2021). While the greyscale images best visualize breaks in the data, and are particularly useful in tracing the appropriate location of structures, the coloured images together with the multi-scale edges give an appreciation of the dip direction and dip estimate of particular magnetic horizons. The gravity and magnetic multi-scale edges were used for a semi-quantitative interpretation of dip, dip direction and penetration depth of main structures in order to differentiate between major and minor shear zones. This broad structural framework was then iteratively fine-tuned during the smaller-scale interpretation stages. The semi-quantitative estimate of the dip and dip direction of a particular magnetic horizon or structures was further achieved by interpreting gradients in the magnetic data using aeromagnetic images processed with either a sun overhead illumination or no sun illumination.

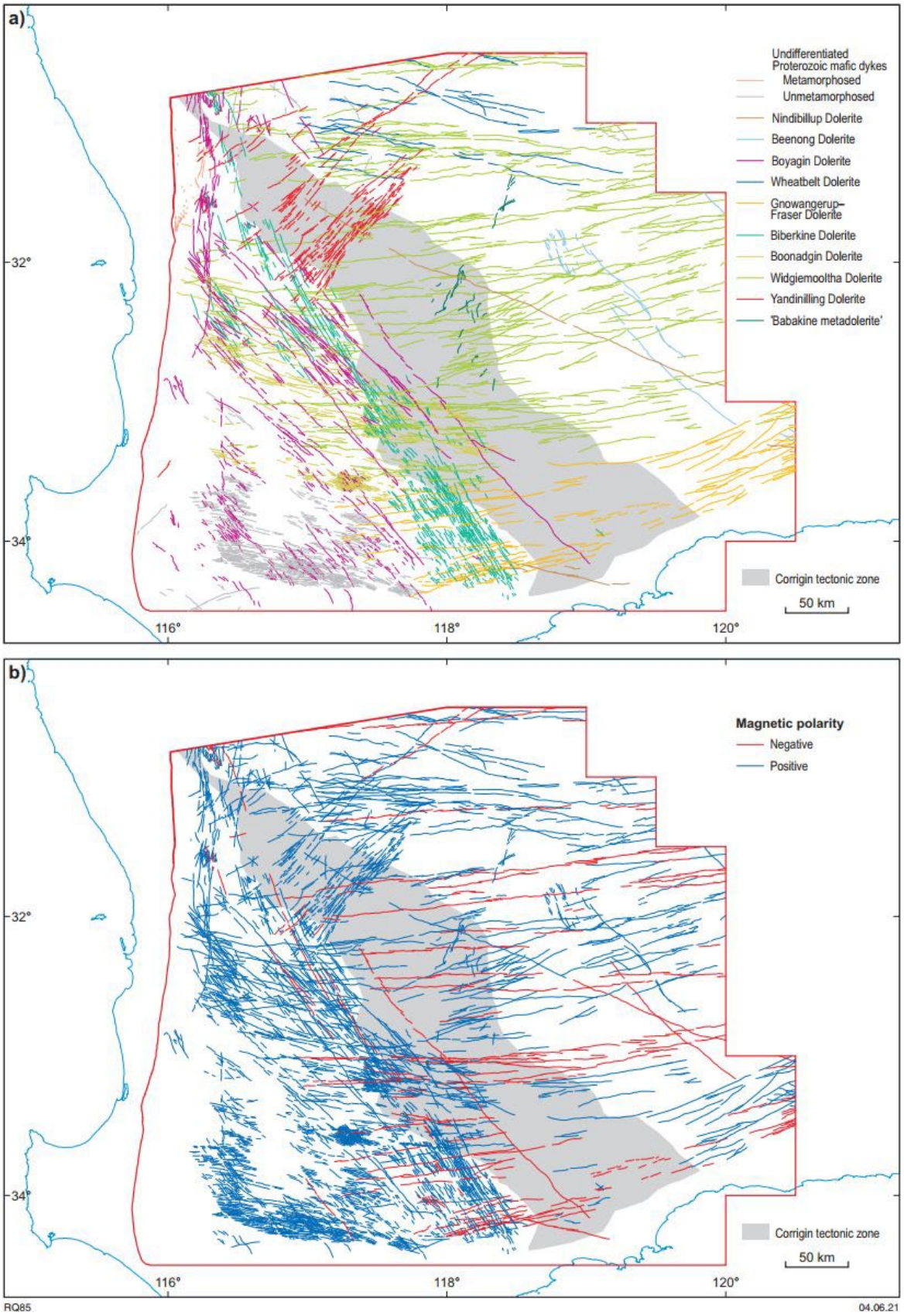

Figure 2. Interpreted mafic dykes: a) colour-coded by name (inverted commas indicate informal name); b) colour-coded by magnetic polarity

A total of 3868 structural lines were interpreted and digitized into the structural line layer ('Interpreted pre-Mesozoic bedrock geology structural lines, 2021'). The very large majority of structural lines were attributed as either 'fault' or 'shear zone' (see below). The few structures attributed as 'fault or shear zone' are a relic from the pre-existing mapping copied into this data package for edge matching purposes and thus only occur on the periphery of the map. Where constraints are known, faults and shear zones are also attributed with dip estimates, dip direction and kinematic attributes as well as maximum and minimum ages. The age constraints were interpreted from crosscutting relationships of dated geological features, where known. As a result, the structures can be symbolized or colour-coded by structure type or kinematics but also by minimum and/or maximum age (Figs 3–5).

Shear zones

Care was taken to differentiate shear zones from faults. For a shear zone to be mapped from aeromagnetic data, it needs to fulfil at least some first-order criteria: they must be wide zones, anastomosed, show curved offsets of magnetic horizons and rotations of magnetic elements towards parallelism, which indicates the high strain portion of the shear zone. They also need to fulfil at least some of the following second-order criteria: show evidence of truncation, folding, attenuation, boudinage and/or magnetite remobilization. Although, a shear zone is defined as a zone of heterogeneously distributed strain relative to its wallrock, the current layer structure for the interpreted bedrock geology requires the structures to be drawn as lines, it was chosen to place the line where truncations occur or where the highest strain portions of the shear zones are interpreted to occur as defined and evidenced by the aeromagnetic form lines mentioned above.

Faults

To satisfy the interpretation of a structure as a fault from the magnetic data alone, the mapped features need to display at least some of the following characteristics; they need to be thin, linear features showing straight offsets, mostly represented by demagnetized zones, locally with a weak and diffuse magnetic response possibly due to minor magnetite/hematite remobilization along the fault. Observations from aeromagnetic interpretation suggest that the faults can act as a propagation medium but also as a barrier to dyke emplacement. As a result, careful, meticulous, and systematic mapping of each fault–dyke intersection was required to assign with some degree of confidence a relative timing between the mapped fault sets and dyke suites and their members. It should be noted that in this interpreted bedrock geology map, only the faults with a cumulative displacement visible in the available magnetic resolution data were mapped, and no attempt has been made to map fracture patterns.

Folds

Fold interpretation from aeromagnetic data was achieved using the principles of structural geophysics (Jessell 2001), using coloured aeromagnetic images processed with either a sun overhead illumination or no sun illumination such as 'SWYC_tmi_RTP_drape90_ps' or 'SWYC_tmi_RTP_colour_ps'. This allows for the semi-quantitative estimate of the dip angle and dip direction of the folded magnetic horizon to be interpreted, as a result one may be able to differentiate between antiforms and synforms, estimate folds interlimb angle and interpret fold orientation, plunge and vergence. These features are attributed where they could be estimated with reasonable confidence.

Structure maps

Because of the way individual lines from the structure line layer are attributed, it is possible to distinguish ductile structures from brittle structures; and by plotting only the interpreted geophysical lines, together with the structures attributed as shear zones, one can obtain a map of the ductile fabrics alone (Fig. 3). Similarly, one can map the brittle structures alone (Fig. 4). The maximum and minimum ages of the structures, interpreted from crosscutting relationships to dated geological units (polygons or lines), could be assigned to about half of all the structure lines and colour-coded according to minimum or maximum ages resulting in a basic structural evolution diagram (Fig. 5).

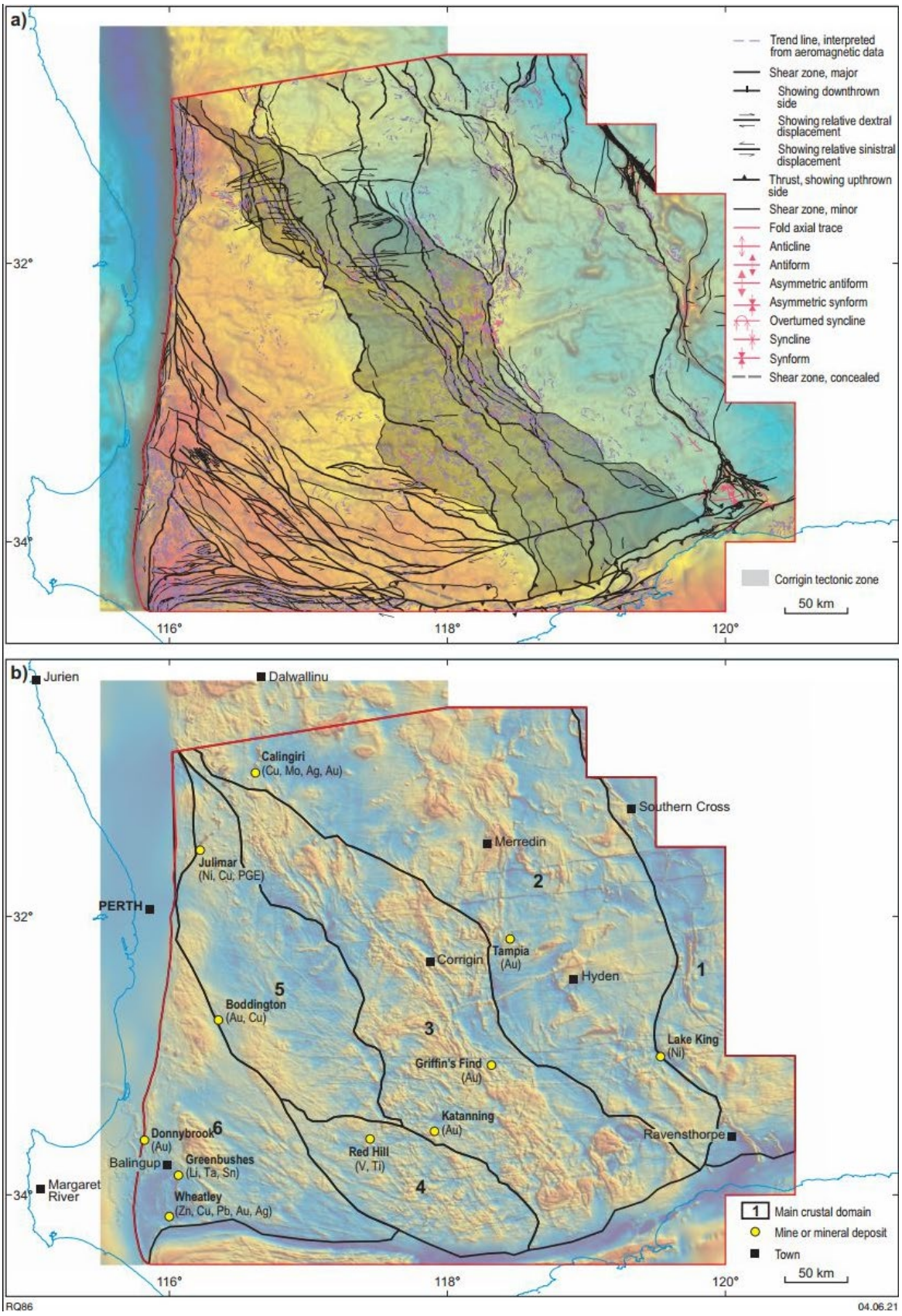

Figure 3. a) Interpreted ductile structures of the southwest Yilgarn displayed over the Bouguer gravity compilation image. The dashed blue lines are form lines interpreted from aeromagnetic data; b) Main crustal domains displayed over the upwards continued (500 m), RTP total magnetic compilation image

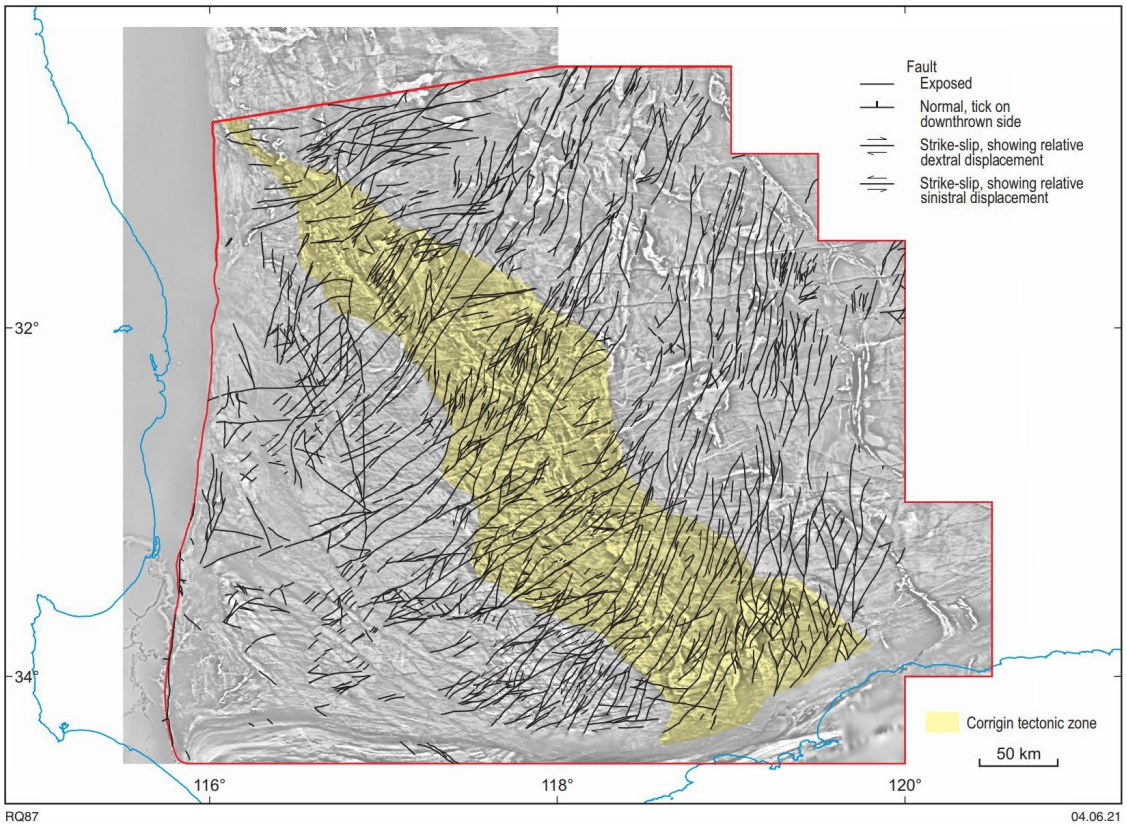

Figure 4. Interpreted brittle structures of the southwest Yilgarn displayed over the upwards continued (500 m), first vertical derivative, RTP total magnetic compilation image

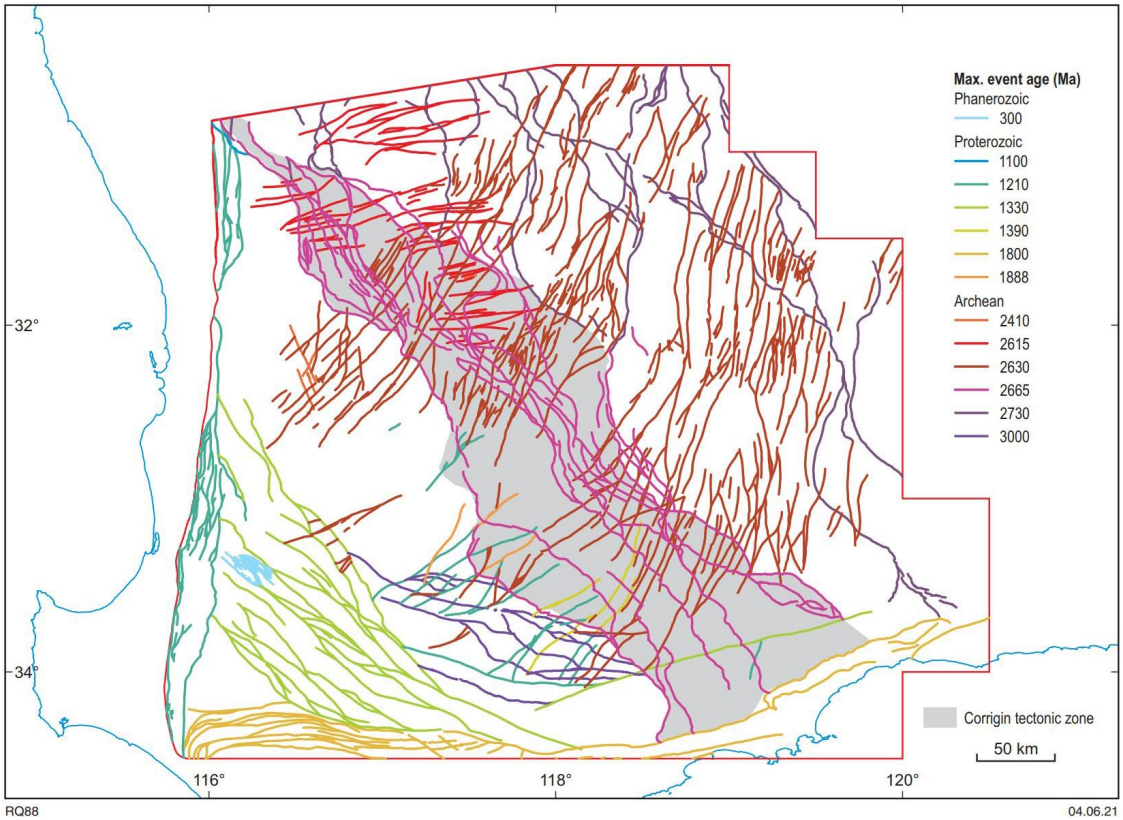

Figure 5. Structures with age data attribution of the southwest Yilgarn colour-coded by maximum age. Thirteen age brackets were defined based on cross-cutting relationships with dated geological units (see text for explanation)

Based on this approach and on crosscutting relationships, we defined 13 relative age brackets for movement along faults and shear zones:

i. 3000–2665 Ma: major west-northwesterly trending shear zones between the Katanning Au region (Fig. 1) and the Albany–Fraser Orogen, and restricted to the South West Terrane. The maximum age is not constrained, only generally attributed to the oldest known gneissic granite in the map area. The minimum age constraint is the maximum age of the Corrigin Tectonic Zone, which truncates the west-northwesterly trending shear zones.

ii. 2730–2665 Ma: major approximately north-striking anastomosing shear zone system of the Youanmi Terrane (i.e. lozenges). The maximum age is that of the earliest age of deformation for the Yilgarn orogeny of Zibra et al. (2017). The minimum age constraint is the maximum age of the Corrigin Tectonic Zone, which truncates and drags sinistrally the north-striking lozenges of the Youanmi Terrane.

iii. 2665–2635 Ma: major northwest-striking sinistral transpressive shear zone system of the Corrigin Tectonic Zone (see Domain 3 of 'Crustal Domain' section below). The maximum and minimum age constraints are defined by the oldest and youngest metamorphic zircons in the Corrigin Tectonic Zone, which also encompass the age range obtained from monazite.

iv. 2630–2410 Ma: prominent set of northeast-striking faults, some individual faults exceeding 200 km, mostly showing dextral shear sense, and cutting across the South West and Youanmi Terranes. These faults affect low-Ca granite plutons dated at c. 2630 Ma but pre-date the c. 2410 Ma Widgiemooltha Dolerite. These faults could therefore be of similar age to the c. 2615 Ma Yandinilling Dolerite dykes.

v. <2615 Ma: east-northeasterly striking shear zones in the northern part of the map affecting the Corrigin Tectonic Zone structures and the c. 2615 Ma Yandinilling Dolerite dykes. No minimum age constraint could be defined.

vi. <2410 Ma: minor set of northwest-striking faults, mostly dextral, restricted to the South West Terrane and affecting the 2410 Ma Widgiemooltha Dolerite.

vii. 1888–1390 Ma: minor set of dominantly sinistral faults affecting the c. 1888 Ma Boonadgin Dolerite dykes but not affecting the c. 1390 Ma Biberkine Dolerite dykes.

viii. 1800–1140 Ma: major east-striking shear zones of the Albany–Fraser Orogen. The maximum age for these shear zones is interpreted to be related to extensional faulting that formed the c. 1800–1590 Ma Barren Basin and the minimum age is likely related to deformation during the c. 1225–1140 Ma Stage II of the Albany–Fraser Orogeny.

ix. <1390 Ma: minor set of mostly sinistral northeasterly to north-northeasterly striking faults, restricted to the southern part of the map area and truncating the redefined terrane boundary between the South West and Youanmi Terranes, affecting the c. 1390 Ma Biberkine Dolerite dykes.

x. 1330–1140 Ma: major northwesterly trending, sinistral, ductile shear zones, restricted to the southern part of the South West Terrane, in the southwestern corner of the map area. These shear zones are interpreted to be Proterozoic in age, as they affect the c. 2610 Ma granites, and are possibly synchronous with compressional or transpressional deformation related to the c. 1390–1140 Ma Albany–Fraser Orogeny. Alternatively, they may be related to the early stages of sinistral transtensional deformation producing the north-trending fabric along the Darling Fault scarp (Zibra, 2021) and the regional-scale sinistral drag of tectonic fabrics of the western end of the western Albany–Fraser Orogen; however, they are truncated by the latest stages of north-trending fabrics parallel to the Darling Fault.

xi. <1210 Ma: minor set of mostly sinistral northeast-trending faults restricted to the South West Terrane affecting the c. 1210 Ma Boyagin Dolerite dykes that probably reactivated the c. 2630–2410 Ma faults of the same orientation.

xii. <1210 Ma: major set of north-trending structures parallel to the Darling Fault scarp, produced during sinistral transtension as identified in the Chittering Metamorphic Belt (Zibra, 2021) and likely producing the regional-scale apparent sinistral drag of tectonic fabrics of the western end of the western Albany–Fraser Orogen. These structures deform north-trending dolerite dykes attributed to the 1210 Ma Boyagin Dolerite suite providing a maximum age of deformation for the sinistral transtensional event. The minimum age is unknown.

xiii. <299 Ma: mostly northwest-trending faults affecting the Carboniferous–Permian Collie Sub-basin in the southwest part of the map that likely reactivated the pre-existing c. 1330–1140 Ma major northwesterly trending, shear zones in the area.

Geology polygons

A total of 1581 polygons were interpreted and digitized into the geology polygon layer ('Interpreted pre-Mesozoic bedrock geology polygons, 2021'). Each polygon is attributed with a code, a unit name, a description, and where available, with maximum and minimum ages and granite geochemistry classification. The main datasets utilized were the WAROX observations (GSWA, 2020a) and WAROX text searches (Ivanic et al., 2021a), the granite geochemistry classification (Smithies et al., 2021), company and GSWA mafic geochemistry, particularly the MgO content to differentiate between mafic and ultramafic rocks (Ivanic et al., 2021b), GSWA zircon U–Pb geochronology data (GSWA, 2020b), external geochronology, GSWA 1:250 000 surface geology maps, MINEDEX Mines and Mineral deposits layers (GSWA, 2021), and various company maps (GSWA, 2021). All these data were integrated and assembled in a uniform interpretation using compilation images of the aeromagnetic and gravity data (GSWA, 2021).

The outlines of the polygons were digitized primarily using various compilation images of the aeromagnetic data, by defining domains of similar texture and intensity. The tilt image ('SWYC_tmi_Tilt_drape_ps') image is particularly useful to delineate areas of similar texture. The various clipped images ('SWYC_tmi_RTP_clipped') were largely used in areas of overall low magnetic intensity to reveal magnetic features otherwise masked by a colour stretching of the aeromagnetic data over too large a range of values. The point datasets were correlated to the combined characteristics of aeromagnetic domains and gravity response (high, medium or low) and the correlation between point data and potential field data was primarily achieved in areas of high point data density. The resulting interpretations were then extrapolated in areas or lesser point data density using primarily the potential field data.

Granites

The extensive granite geochemistry dataset and the resulting granite classification (Smithies et al., 2021) formed the basis for an interpreted granite map. Together with WAROX lithological descriptions, it has been possible to assign aeromagnetic and gravity characteristics for mappable domains of similar geochemical groupings in the aeromagnetic data. The resulting interpretation developed in areas of the highest point data density was then extrapolated to geophysical domains of similar characteristics but with lesser point data density. Each granite polygon was attributed to a particular granite group, allowing the compilation of a granite map (Fig. 6). However, small granite plutons of specific granite class, such as sanukitoids, were not captured as single polygons, because it was not possible to individually map polygons from the resolution of the geophysical datasets. As a result, these have been included as minor components within a composite polygon, with the various lithologies present expressed in the legend narrative.

The seven granite geochemical groups represented on the interpreted bedrock geology map are:

i. High Ca, Na to high Na, high Sr/Y: largely consisting of metamorphosed, foliated to gneissic, locally migmatitic tonalite–trondhjemite–granodiorite (TTG). These typically have a low to medium gravity response, low to moderate magnetic intensity and are textureless. In the informal Lake Grace terrane of Wilde et al. (1996), they form an extensive area with a distinctive, shear zone-bounded, oblong crustal domain, similar to lozenge-shape domains in the northern part of the Youanmi Terrane. The TTGs intrude into greenstones of the Youanmi Terrane, where the greenstones form dismembered rafts 'floating' in a 'sea' of high-Ca granite.
ii. High Ca, Na, low Sr/Y: typically hornblende granodiorite, mostly occurring within the South West Terrane as relatively undeformed intrusions, except for areas of Proterozoic deformation along the Darling Fault scarp.
iii. High Ca, and not further differentiated, either because of insufficient data points or because mixed high and low Sr/Y was not possible to differentiate as unique polygons.
iv. High Ca, K, high Sr/Y: rare occurrences within the Corrigin Tectonic Zone consisting of migmatitic, gneissic TTG.
v. High Ca, K, low Sr/Y: rare occurrences in the northwest corner of the map area of metamorphosed hornblende-bearing granodiorite to monzogranite.

vi. Low Ca, K, low to high Sr/Y: typically weakly foliated porphyritic biotite monzogranite, commonly forming low-density features within the high-Ca granites with moderate magnetic intensity and a well-developed mottled texture. The c. 2677–2610 Ma low-Ca granites were emplaced synchronously with the c. 2665–2635 Ma deformation and metamorphism of the Corrigin Tectonic Zone. In the Corrigin Tectonic Zone, they occur as sheets emplaced along the footwalls of ductile shear zones; however, their occurrence is not restricted to the Corrigin Tectonic Zone. In the northern part of the map area, outside of the Corrigin Tectonic Zone, they form plutons often emplaced at a triple junction between earlier ductile structures and seem to inflate, overprint and cross-cut these structures. These are interpreted as post-tectonic granites, post-dating the north-trending shear zone system attributed to result from c. 2730–2660 Ma deformation. They also occur as domes within large areas of high-Ca granite, for example, the low-Ca granite pluton exposed at Wave Rock. The emplacement of the low-Ca granite is therefore not the result of orogenesis in the Corrigin Tectonic Zone, but more likely related to a thermal event superimposed and potentially fortuitously synchronous to c. 2665–2635 Ma deformation and metamorphism in the Corrigin Tectonic Zone.

vii. Dominantly low Ca, P-rich: commonly monzogranite and syenogranite, rarely granodiorite, typically biotite-bearing and forming high magnetic intensity areas, with a well-developed mottled texture, of low to moderate density. These appear as cogenetic with the low-Ca granites but possibly as later P-rich phases within a low-Ca intrusion cycle. Where they occur in the Corrigin Tectonic Zone, they appear intruded as sheets directly against and along the footwalls of the shear zones and are interpreted as syntectonic granite. Outside of the Corrigin Tectonic Zone, they form concentric zonation with the low-Ca, K, low-Sr/Y group described above and seem to inflate existing post-tectonic low-Ca granites overprinting existing deformation structures.

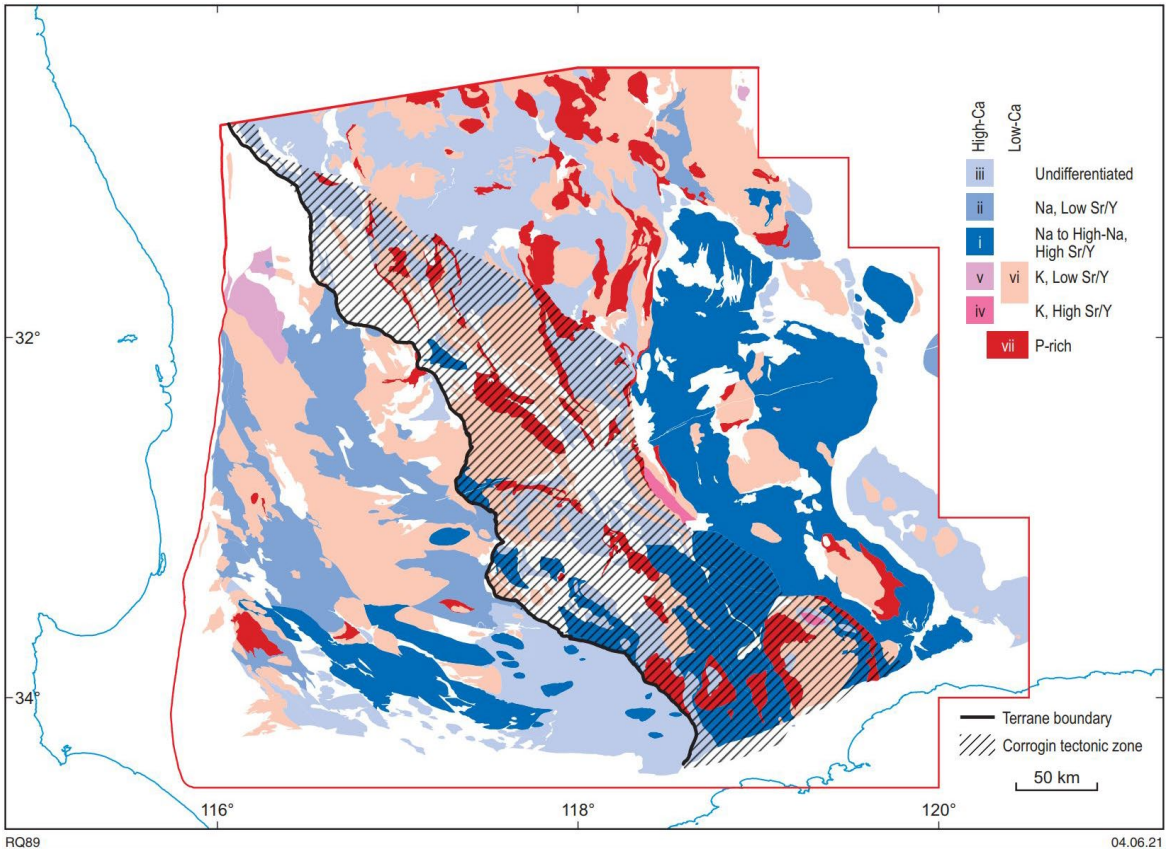

Figure 6. Interpreted granite map of the southwest Yilgarn showing the distribution of mappable polygons of major geochemical granite groups. Roman numerals in legend refer to text

Greenstones

The dominant datasets used in differentiating polygons and lines of greenstone lithologies were the WAROX database, existing surface mapping (GSWA and external), aeromagnetic texture and intensity and gravity response. The greenstone geochemistry dataset (Ivanic et al., 2021b), is highly focused on isolated drillcore samples, thus it was locally very useful for lithological assignment. The geochemical point data were classified into various geochemical groups and classes and, in a few instances in this interpreted bedrock geology map, it has been possible to assign greenstones based upon these groups.

We assigned greenstone polygon codes either to the South West Terrane or the Youanmi Terrane (i.e. A-lithology-YSW or A-lithology-YYO), and this decision was based primarily on geochronological constraints. For example, the South West Terrane, as we define it, has distinctly younger greenstone depositional ages than the Youanmi Terrane. Mixed lithology codes were used in many instances in both terranes to represent heterogeneous map units or units with fine interlayering. For example, where metasedimentary and metabasaltic rocks were interpreted to be interlayered and lensed together along shear zones, or where abundant metamonzogranite sheets intrude amphibolite.

Even though the terrane boundary itself was drawn along interpreted structures that post-date greenstone deposition, the boundary does appear to separate polygons of distinct greenstone characteristics.

Without a direct record of lithology in the WAROX database, the following list summarizes the ways we differentiated the main groups of greenstones (including their metamorphosed equivalents) in both terranes on the interpreted bedrock geology map:

- Ultramafic volcanic rocks: highly magnetic (typically narrow trend lines), high density, interlayered with mafic volcanic rocks and metasedimentary rocks, generally <45 wt% SiO_2, >18 wt% MgO.
- Mafic volcanic rocks: generally, low magnetic response, moderate density, interlayered with metasedimentary rocks, locally intruded by sills of mafic–ultramafic intrusive rocks, 45–57 wt% SiO_2; <18 wt% MgO.

- Felsic–intermediate volcanic rocks: typically too thin to show a distinct geophysical response, >57 wt% SiO_2.
- Ultramafic intrusive rocks: generally highly magnetic (wider, elongate, irregular shapes compared to BIF), high density, MgO > 18 wt%; often in a belt containing several small circular features; where metamorphosed to high grade, they tend to form ovoid features, 1–10 km across.
- Mafic intrusive rocks: generally low–moderate magnetic intensity, moderate–high gravity response, 6–18 wt% MgO; where Fe rich, they are highly magnetic due to interlayered gabbro and magnetitite; where metamorphosed to high grade, they tend to form ovoid features.
- Siliciclastic sedimentary rocks: generally low magnetic intensity, featureless and low density.
- Chemical sedimentary rocks: extremely highly magnetic, typically thin, narrowly spaced magnetic lines, high density, typically interlayered with mafic volcanic rocks; chert-rich rather than BIF-rich successions are typically too thin to show a distinct geophysical response.

These results are shown in a greenstones map for the interpreted bedrock geology extent (Fig. 7). The lithological assemblages vary across the map and form northwest-trending domains. From southwest to northeast these informal assemblages are:

- Assemblage 1: Greenstone belts at Forrestania, Lake King and Ravensthorpe (Fig. 1) have lithological assemblages more typical of Neoarchean Youanmi Terrane greenstone belts with ultramafic volcanic rocks, mafic volcanic and intrusive rocks, metasedimentary siliciclastic rocks and BIF. Lower proportions of felsic–intermediate volcanic rocks and ultramafic intrusive rocks.
- Assemblage 2: Greenstone belts at Wongan Hills, Westonia and Holleton have lithological assemblages more typical of Mesoarchean Youanmi Terrane greenstone belts with high proportions of each of: mafic volcanic, mafic intrusive rocks and both metasedimentary siliciclastic rocks and BIF and lower proportions of felsic–intermediate volcanic and ultramafic volcanic rocks.
- Assemblage 3: Greenstones in a wide area centred on Narembeen (and similar to the Corrigin Tectonic Zone structural domain) have lithological assemblages comprising granulite-facies mafic intrusive, mafic volcanic and sedimentary rocks and lesser ultramafic rocks. This is more typical of Mesoarchean Youanmi Terrane greenstone belt assemblages, but at higher metamorphic grade.
- Assemblage 4: Greenstones in the Northam area have lithological assemblages comprising BIF interlayered with metamorphosed siliciclastic, mafic volcanic and mafic intrusive rocks. This is similar to Mesoarchean Youanmi Terrane greenstone belt assemblages, but with a higher abundance of metasedimentary rocks.
- Assemblage 5: In the north and east of the South West Terrane the majority of greenstones comprise metamorphosed siliciclastic rocks intruded by mafic–ultramafic sills and plugs.
- Assemblage 6: The Boddington greenstone belt comprises a distinct lithological assemblage of mafic–intermediate volcanic rocks and lesser metasedimentary rocks and ultramafic sills.
- Assemblage 7: In the far west and south of the South West Terrane, the area coincident with the 'Balingup terrane' (Wilde et al., 1996) contains dominant siliciclastic rocks locally with numerous small ultramafic sills.

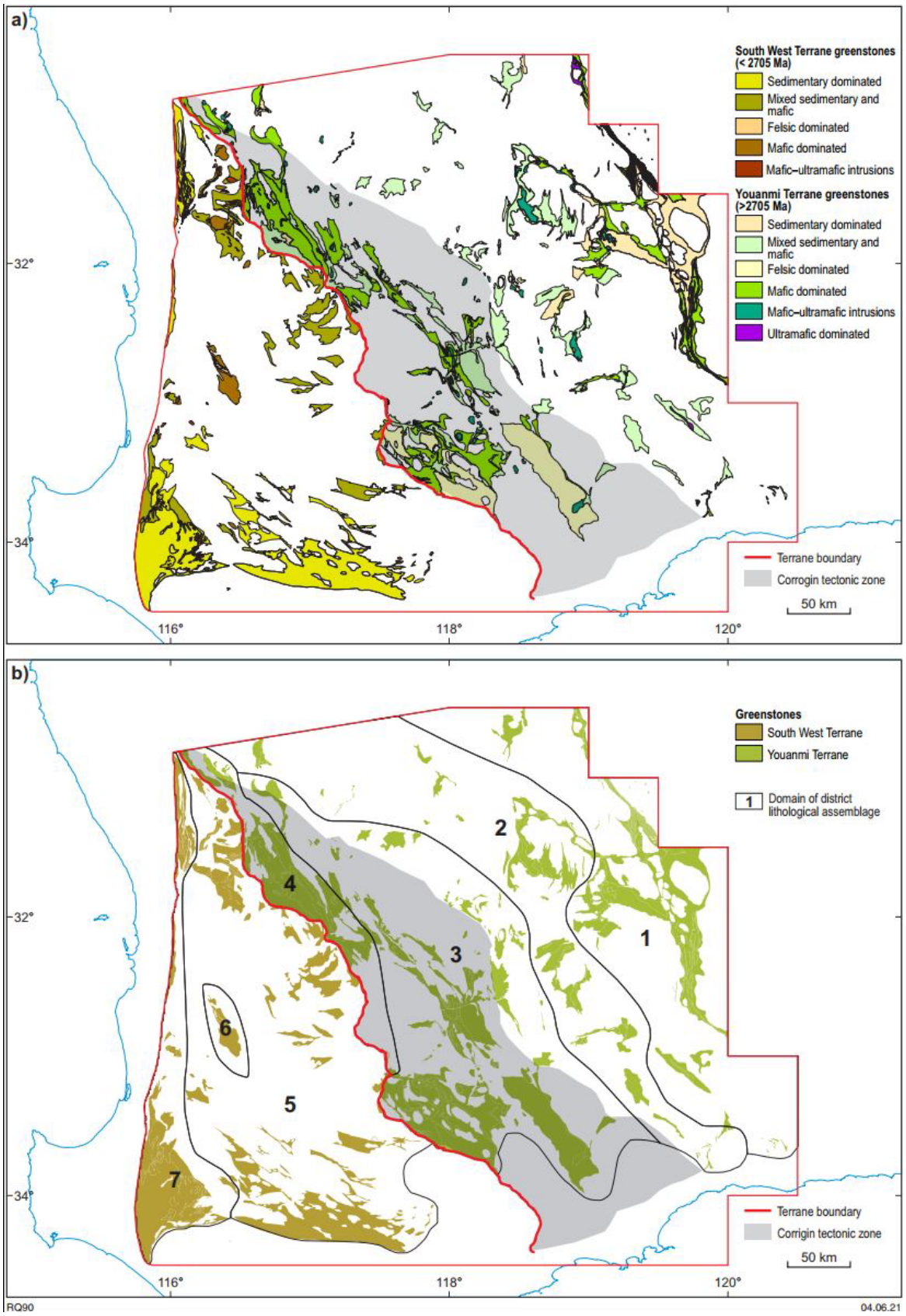

Figure 7. Interpreted greenstone map groups of the South West Terrane and the southwestern Youanmi Terrane. Inset shows numbered domains of distinct lithological assemblages (see text for explanation)

Main findings

Crustal domains

We identify six main shear zone-bounded crustal domains of different geological history across the interpreted bedrock geology area (Fig. 3b); these are:

Domain 1: A greenschist to amphibolite facies domain within the Youanmi Terrane, bounded to the west by the Youanmi Shear Zone. This domain includes characteristic linear and fault-bounded greenstone belts such as Southern Cross, Forrestania, Lake King and Ravensthorpe (Fig. 1). These are intruded by large granitic domes that dominantly show regional-scale sinistral asymmetry.

Domain 2: An amphibolite- to granulite-facies domain within the Youanmi Terrane, bounded to the east by the Youanmi Shear Zone and to the west by the Corrigin Tectonic Zone. This domain contains a shear zone system that anastomoses and forms lozenges of similar shapes and probably of similar geological history to the 2730–2665 Ma north-trending lozenges observed further north in the Youanmi Terrane; however, here the long axes of the lozenges trend north-northwest. This change in orientation from northerly to north-northwesterly trending is interpreted to result from rotation of the long axes of the lozenges (simple shear component) during sinistral drag along the eastern margin of the 2665–2635 Ma sinistral transpressive Corrigin Tectonic Zone (see Domain 3). Domain 2 is largely dominated by gneissic TTGs with high Ca, ±Na and high Sr/Y values (Fig. 6) intruded into Youanmi greenstones. The greenstone associations in this domain occur as dismembered rafts within the gneissic TTGs. Minor porphyritic low-Ca, K, low-Sr/Y biotite monzogranite, such as that observed at Wave Rock near Hyden (Figs 1, 6), form domes within the gneissic TTGs. This domain is interpreted to represent a mid-crustal level exposure.

Domain 3 (the Corrigin Tectonic Zone): A strongly deformed, largely migmatitic, granulite-facies domain forming the southwestern end of the Youanmi Terrane. The area contains a moderately to steeply northeast-dipping foliation, shows abundant tight to isoclinal folds that are dominantly west-verging, and commonly display regional-scale asymmetric boudins indicating sinistral shear sense. The deformation is interpreted to be partitioned into moderately northeast-dipping thrusts and steeply dipping, northwest-striking sinistral shear zones that we interpret to have formed in between 2665 and 2635 Ma. The area hosts a high proportion of migmatitic, gneissic TTGs intruded by syntectonic low-Ca, K, low-Sr/Y and low-Ca, P-rich metamonzogranite and metasyenogranite intruded as tabular sheets along and in the footwalls of northwest-striking shear zones of the Corrigin Tectonic Zone (Fig. 6). The counter clockwise rotation of the lozenges' long axes of Domain 2 along the Corrigin Tectonic Zone, together with the identification of regional-scale, northwest-trending, asymmetric sinistral boudins, and of compressional southwest-verging tectonic fabrics, indicates that deformation was partitioned into moderately northeast-dipping thrusts and steeply dipping, northwest-striking sinistral shear zones. These observations form a strong argument that the Corrigin Tectonic Zone resulted from sinistral transpression. The Corrigin Tectonic Zone is dominated by migmatitic rocks that generally record metamorphic conditions of 5–7 kbar and 700–900 °C, although lower and higher values are also reported (Korhonen et al., 2021). The U–Pb zircon and monazite metamorphic ages for this zone are between c. 2665 and 2635 Ma, interpreted as the age of high-grade metamorphism and likely as the age of deformation. Zircon $\delta^{18}O$ values from c. 2800 to 2641 Ma granitic rocks from the Corrigin Tectonic Zone yielded values ranging between 6.5 and 6.9‰ (Lu et al. 2021b) suggesting significant tectonic burial of supracrustal material into the source region of the c. 2800 to 2641 Ma granite, which is consistent with the underthrusting inferred from the transpressional interpretation for the Corrigin Tectonic Zone.

Domain 4: Potentially a relatively old and deep crustal domain within the otherwise apparently younger South West Terrane. The basement aeromagnetic features within this domain are largely obscured by the very high density of northwesterly to north-northwesterly striking mafic dykes. Mapping the aeromagnetic form lines in the background of these dykes revealed a systematic west-northwesterly striking domain. West-northwesterly trending ovoid features in this domain with concentric aeromagnetic trend lines and associated with high-Ca, high-Na, and high-Sr/Y granite analyses are interpreted as ovoid TTG plutons (Fig. 6). Major west-northwesterly trending shear zones bound and occur within this domain and are interpreted to pre-date and control the emplacement of the TTG plutons dated at c. 2702 Ma and c. 2669 Ma and are truncated by the northwest-striking major shear zones of the 2665–2635 Ma Corrigin Tectonic Zone. The shear zones bounding this domain control the distribution of exposed high-Ca granites with high Sr/Y values in the South West Terrane. Domain

4 is largely dominated by TTGs with high Ca (± Na) and high Sr/Y, while the high-Ca (± Na) granites of Domains 5 and 6 have almost exclusively low Sr/Y values. Additionally, Domain 4 contains very few low-Ca granites while Domains 5 and 6 are largely dominated by them. Domain 4 also coincides with a high gravity anomaly and we interpret the basement into which the TTG plutons were intruded as a mixed intermediate and mafic gneissic crust, which possibly represents a low crustal level exposure. One major west-northwesterly trending shear zone in this domain is spatially associated with sanukitoid and low-Ca, high-P intrusions and has been found to host Au occurrences. The west-northwesterly trending structures of Domain 4 have likely been reused during the intrusion of the west-northwesterly trending c. 1888 Ma Boonadgin Dolerite dykes.

Domain 5: A domain largely dominated by low-Ca, K, low-Sr/Y biotite monzogranite, a large area of hornblende-bearing granodiorite and minor high-Ca (±Na) granite exclusively with low Sr/Y values. This domain is bounded to the east by the Corrigin Tectonic Zone and to the west by Proterozoic shear zones of the proto-Darling Fault and also includes Julimar (Ni) and Boddington (Au) (Figs 1, 3b). Although unconstrained, the overall metamorphic grade of Domain 5 appears lower than that of the Corrigin Tectonic Zone (i.e. Domain 3); indeed the rock succession at Boddington is at greenschist facies. We interpret this domain as an upper crustal level exposure.

Domain 6: This domain is bounded to the west by the Darling Fault and to the south by the Albany–Fraser Orogen. It includes the Chittering Metamorphic Belt, as well as the sedimentary succession around Balingup and hosts REE-bearing pegmatite at Greenbushes (Figs 1, 3b). It is mainly characterized by the widespread Proterozoic overprint that produced the numerous major shear zones that dissect this domain, either as north-striking shear zones subparallel to the Darling Fault or as closely-spaced, northwest-trending shear zones in the southwest corner of the map area. This domain contains a larger proportion of sedimentary rocks than any other domain, and also contains a young 2615–2610 Ma suite of granite.

Redefined boundary between the Youanmi and South West Terranes

Three significant issues were identified with the previous terrane boundary between the Youanmi and South West Terranes of Cassidy et al. (2006), which:

- cuts geophysical trend lines at a high angle
- does not differentiate between crustal domains with contrasting geological histories
- does not represent a change in lithological assemblages within greenstone belts.

In our new interpretation, the Youanmi Terrane has been extended southwest to include Domain 2, which broadly coincides with the informal Lake Grace terrane of Wilde et al. (1996) and the Corrigin Tectonic Zone (i.e. Domain 3; Figs 1, 3). The terrane boundary with the South West Terrane is now interpreted to lie along the southwestern deformation front of the northwest-trending Corrigin Tectonic Zone, which, together with the informal Lake Grace terrane, are now interpreted to represent an upper amphibolite to granulite facies equivalent to the rest of the Youanmi Terrane. Key variations within many new or updated datasets (Fig. 8) were used to guide interpretation of the new terrane boundary: Nd and O isotopes, the distribution of igneous crystallization ages, the nature of the greenstone belts, mineralization data, granite geochemistry, structural patterns, deformation style and metamorphic history data. Regarding the metamorphic data, nearly all new pressure and temperature data are from samples within the amphibolite- to granulite-facies Youanmi Terrane, but it is clear that there has to be a significant change towards the western portion of the South West Terrane because supracrustal rocks at Boddington have been identified to be at greenschist facies. Among these datasets, the geochronology of granite and greenstone samples was the one that most clearly differentiated the two terranes.

We have identified that Domain 2 is characterized by an anastomosed system of north-northwesterly striking shear zones that collectively form lozenge-shape patterns that closely resemble those of the central and northern parts of the Youanmi Terrane (Fig. 3). The similar lithological associations and geochronology data between Domain 2 and the rest of the Youanmi Terrane strongly suggests that the lozenge patterns affected similarly aged rocks to those in the rest of the Youanmi Terrane, indicating that they also formed during tectonic events occurring between 2730–2665 Ma (Zibra et al. 2017). The lack of lozenge shear zone patterns in the South West Terrane marks a strong difference in structural style and suggests that it shares a different tectonic history.

Similarly, the zircon O isotopes also indicate that the South West Terrane and the Youanmi Terrane did not experience the same tectonic history (Lu et al. 2021b). The South West Terrane contains zircon

dominated by mantle-like $\delta^{18}O$ values (4.7 – 5.9‰), indicating that no significant supracrustal reworking has occurred prior to or during granite generation. By contrast, values from the Youanmi Terrane commonly have $\delta^{18}O$ values over 5.9‰ suggesting at least a minor amount of crustal reworking and supracrustal material burial into the source regions of granites of the amphibolite- to granulite-facies portion of the Youanmi Terrane. The highest zircon O isotopes values ($\delta^{18}O$ up to 6.9‰) in the whole Yilgarn Craton have been obtained from granitic rocks along the proposed terrane boundary between the South West and the Youanmi Terranes, possibly indicating that maximum burial of supracrustal material has occurred along this boundary.

The Nd isotope depleted mantle model age (T_{DM2}) map of the project area indicates an overall change to younger model ages (<2.95 Ga) across the terrane boundary towards the southwest, but the shift is not distinct (Lu et al. 2021a). There are several regions within the South West Terrane with >3 Ga Nd model ages, which is similar to the Youanmi Terrane. However, the overall texture of the isotopic map does change to the southwest whereby the domains of similar ages are much smaller. This pattern within the South West Terrane may indicate local Youanmi Terrane basement such as in the area around Boddington, but also a different geological history involving multiple, younger, juvenile input events, which are not known from the Youanmi Terrane.

Magmatic crystallization ages within granitic rocks indicate that >2.8 Ga granitic rocks are restricted to the Youanmi Terrane. Xenocrystic zircons within granitic rocks show that the oldest grains within the South West Terrane are c. 2.8 Ga, whereas 2.9 – 3.1 Ga xenocrystic zircons are widely present in granitic rocks of the Youanmi Terrane (Fig. 8).

Magmatic crystallization ages constraining the age of deposition and mafic magmatism within greenstones differ across the new terrane boundary. Figure 8 shows that the Youanmi Terrane experienced a distinct, older history of greenstone deposition from 2.7 – 3.1 Ga, compared to 2.7 – 2.4 Ga in the South West Terrane. The c. 2.69 Ga 'McCaskill group' in the Youanmi Terrane is very localized and occurs as very low volume slivers, whereas the 2704–2670 Ma Saddleback Group in the South West Terrane is more voluminous and protracted with a higher proportion of volcanic rocks. The 'Balingup supergroup' has poor geochronological constraints:

- Metasandstone at Wheatley has an interpreted maximum depositional age 2646 Ma (Sircombe et al. 2007).
- In the far southwest corner of the South West Terrane, a pelitic gneiss has a 2636 Ma zircon, interpreted as a potential detrital grain (Lu et al. 2015).
- c. 3200 Ma detrital zircons are present in some parts of the stratigraphy (Lu et al. 2016).
- The metasedimentary units to the north are locally cut by a suite of c. 2615 Ma granitic rocks, providing a minimum age constraint.

Thus, while we can say that the 'Balingup supergroup' is different in age (and composition, being very quartzite rich) to anything found in the Youanmi Terrane, further work is required to establish the geological history of the 'Balingup supergroup'.

In terms of mafic–ultramafic intrusive rocks, the geological history of the South West Terrane is independent to the Youanmi Terrane until 2615 Ma (Fig. 8). The 'Julimar' and 'Red Hill' suites at c. 2665 Ma only intrude units of the South West Terrane. Further work is required to test whether these suture across the terrane boundary in the north. If so, they would provide a minimum age for accretion of the two terranes.

Across the project area, the lithological assemblages within greenstones form distinct, northwest-trending domains, where the most significant shift is located at the new terrane boundary between the South West Terrane and the Youanmi Terrane. Overall, this change towards the southwest includes:

- an increase in quartz-rich metasedimentary rocks, including much more abundant quartzite
- an increase in young (c. 2665 Ma), mineralized mafic–ultramafic intrusions
- a decrease in mafic volcanic rocks
- a decrease in BIF
- a decrease in granulite-facies rocks, particularly those with a particularly high thermal gradient (Korhonen et al., 2021).

The revised terrane boundary between the South West Terrane and the Youanmi Terrane represents one of the major divisions within the Yilgarn Craton, second only to the Eastern Goldfields and Youanmi Terrane (Ida Fault). Further work is required to understand the tectonic significance of this boundary and to refine its precise location. Nevertheless, such an important feature provides a crustal-scale (and potentially mantle-tapping) feature to explore for mineral deposits, opening up a corridor of exploration search space.

Stratigraphy, magmatism and mineralization

The reinterpreted terrane boundary presented here indicates a break in the stratigraphy and magmatic history of the South West and Youanmi Terranes (Fig. 8). We consider the new boundary to be a major control on the distribution of several key magmatic suites and stratigraphic units, many of which are mineralized (see details in MINEDEX layer, GSWA, 2021). For example:

- in the South West Terrane:
  - Boddington (Au–Cu–Mo)
  - Julimar (Ni–Cu–PGE)
  - Red Hill (V–Ti)
  - Donnybrook (Au)
  - Wheatley (Zn, Cu, Pb, Au, Ag)
  - Greenbushes (REE)
- and in the Youanmi Terrane (west of the Youanmi Shear Zone):
  - Calingiri (Au–Cu–Mo)
  - Lake King (Ni)
  - Katanning (Au), Tampia (Au) and Griffins Find (Au)
  - iron deposits (Fe), widespread within the Youanmi greenstones.

The magmatism at Boddington, although showing striking similarities with the Kalgoorlie–Kambalda region (Smithies et al., 2021b), is unique in the southwest Yilgarn Craton and we consider it to be a distinct stratigraphic package (in age as well as composition) comprising a higher proportion of intermediate volcanic rocks than anywhere else in the South West Terrane. Further work is required to uncover the total extent of the 'Julimar suite' as we expect several intrusive mafic–ultramafic geological polygons in a wide area of the South West Terrane may be related. Likewise, further work is required to establish the full extent of the 'Red Hill suite', which may occur as sills in a wide area between Katanning and Northam, including the Coates Siding Gabbro (Ivanic et al., 2021b).

The Donnybrook Au deposit is located in the metasedimentary lithological assemblage 7 and we see no reason that similar deposits may exist along strike. At Wheatley, the metasedimentary units hosting mineralization are not exposed and lack of exposure in this part of the South West Terrane means that lithologies and mineralization are essentially unconstrained. The Greenbushes Pegmatite is an outlier in that similar granitic suites are not found in the South West Terrane, but similar rocks may exist in areas under cover.

In the Youanmi Terrane, the c. 3000 Ma, Calingiri mineralization has been linked to particular monzogranite and syenogranite plutons (Outhwaite, 2018) and potentially to the felsic volcanism in the Wongan Hills greenstone belt. The 'Wongan group' and the 'Calingiri suite', part of the Thundelarra Supersuite, are likely to be traceable along a vast area of older Youanmi Terrane greenstones and Yilgarn Craton granitic rocks within the western Yilgarn Craton. In the far northeast of the project area are metamorphosed ultramafic rocks, which, in light of their continuation of the Ravensthorpe – Lake King – Forrestania trend of Ni deposits, are prospective. The Katanning, Tampia and Griffins Find Au deposits lie in proximity to a large volume of granulite-facies mafic–ultramafic rocks. These are exposed in the Corrigin Tectonic Zone and associated structures, often forming circular structures 1–10 km across and interpreted as greenstone 'keels' (e.g. Gee et al., 1986). Immediately north of the terrane boundary, within the southwesternmost Youanmi Terrane, there is a notable linear belt of BIF-hosted Fe deposits (within lithological assemblage 4), but these are typically too thin to yield large deposits.

Conclusion

A pre-Mesozoic interpreted bedrock geology map of the southwest Yilgarn is provided and the wealth of information contained within this map can be displayed in various ways, including mafic dyke maps, structure maps, a granite geochemistry map and a greenstone lithological map. We identify six crustal domains of distinct geological history, also possibly reflecting varying levels of crustal exposure, although further work is required to fully understand this assertion. The most significant outcomes of this work are the redefinition of the terrane boundary between the South West Terrane and the Youanmi Terrane and the ability to provide additional geological background to known deposits of various commodities in the southwest Yilgarn.

The new domains and terranes defined in this work integrate numerous and diverse GSWA and external datasets to present a significantly updated and united geological framework for the southwest Yilgarn. The methodology defined here is capable of dealing with the large and diverse nature of geological data coverage in the Yilgarn. The Pre-Mesozoic interpreted bedrock geology of the southwest Yilgarn, 2021 provides a highly interpreted view of the outcome of this unification process and should be used in parallel with the ~600 geological layers in the Southwest Yilgarn, 2021 Geological Exploration Package (GSWA, 2021). Although further work is required to test and expand this dataset and interpretation of the geological history of the southwest Yilgarn, this work provides a significant leap in geological understanding and can broaden the scope for the exploration of diverse types of mineral deposits.

How to access

The Pre-Mesozoic interpreted bedrock geology map of the southwest Yilgarn is best accessed using GeoVIEW.WA. The digital data are also available as a free download from the Data and Software Centre.

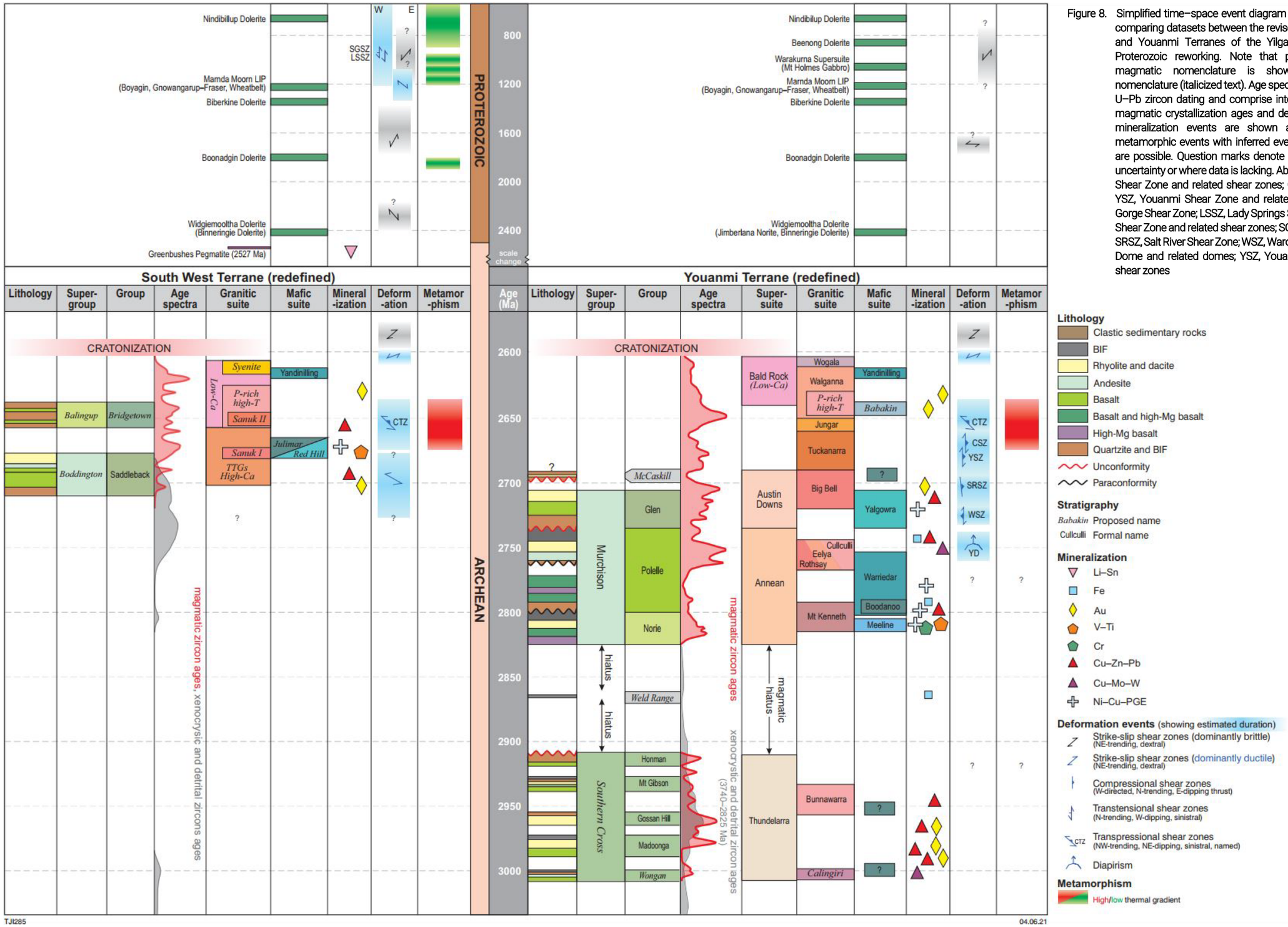

Figure 8. Simplified time–space event diagram and stratigraphic framework comparing datasets between the revised extents of the South West and Youanmi Terranes of the Yilgarn Craton, and subsequent Proterozoic reworking. Note that published stratigraphic and magmatic nomenclature is shown along with proposed nomenclature (italicized text). Age spectra are derived primarily from U–Pb zircon dating and comprise interpreted GSWA and external magmatic crystallization ages and detrital zircon data. Significant mineralization events are shown alongside deformation and metamorphic events with inferred event duration where estimates are possible. Question marks denote features or events with high uncertainty or where data is lacking. Abbreviations: CSZ, Cundimurra Shear Zone and related shear zones; CTZ, Corrigin Tectonic Zone; YSZ, Youanmi Shear Zone and related shear zones; SGSZ, Swan Gorge Shear Zone; LSSZ, Lady Springs Shear Zone; CSZ, Cundimurra Shear Zone and related shear zones; SGSZ, Swan Gorge Shear Zone; SRSZ, Salt River Shear Zone; WSZ, Waroonga Shear Zone; YD, Yalgoo Dome and related domes; YSZ, Youanmi Shear Zone and related shear zones

References

Brett, JW 2021, Multi-scale edges for the southwest Yilgarn from gravity and magnetics: Geological Survey of Western Australia, digital data layer, <www.dmirs.wa.gov.au/geoview>.

Cassidy, KF, Champion, DC, Krapež, B, Barley, ME, Brown, SJA, Blewett, RS, Groenewald, PB and Tyler, IM 2006, A revised geological framework for the Yilgarn Craton, Western Australia: Geological Survey of Western Australia, Record 2006/8, 8p.

Gee, RD, Myers, JS and Trendall, AF 1986, Relation between Archaean high-grade gneiss and granite–greenstone terrain in western Australia: Precambrian Research, v. 33, no. 1, p. 87–102, doi:10.1016/0301-9268(86)90016-1.

Geological Survey of Western Australia 2020a, Compilation of WAROX data, 2020: Geological Survey of Western Australia, Digital Data Package.

Geological Survey of Western Australia 2020b, Compilation of geochronology information, 2020:Geological Survey of Western Australia, Digital Data Package.

Geological Survey of Western Australia 2021, Southwest Yilgarn, 2021: Geological Survey of Western Australia, Geological Exploration Package.

Ivanic, TJ, Kelsey, DE and Duuring, P 2021a, Magmatic and stratigraphic WAROX text search results for the southwest Yilgarn: Geological Survey of Western Australia, digital data layer.

Ivanic, TJ, Lowrey, JR and Smithies, RH 2021b, New geochemical constraints on the mafic and ultramafic rocks of the southwest Yilgarn: Geological Survey of Western Australia, digital data layer.

Jessell, MW 2001, Atlas of Structural Geophysics II: Australian Crustal Research Centre, Journal of the virtual explorer, v. 5. 94p.

Korhonen, FJ, Blereau, ER, Kelsey, DE, Fielding, IOH and Romano, SS 2021, Metamorphic evolution of the southwest Yilgarn: Geological Survey of Western Australia, digital data layer.

Lu, Y, Wingate, MTD, Champion, DC, Smithies, RH, Johnson, SP, Mole, DR, Poujol, M, Zhao, J, Maas, R and Creaser RA 2021a, Samarium–Neodymium isotope map of Western Australia: Geological Survey of Western Australia, digital data layer.

Lu, Y, Wingate, MTD, Smithies, RH, Martin, L, Jeon, H, Champion, DC, Johnson, SP and Mole, DR 2021b, Zircon oxygen isotope map of Western Australia: Geological Survey of Western Australia, digital data layer.

Lu, Y, Wingate, MTD and Bodorkos, S 2016, 184116: quartzite, Polina Road; Geochronology Record 1310: Geological Survey of Western Australia, 4p.

Lu, Y, Wingate, MTD, Kirkland, CL, Goscombe, B and Wyche, S 2015, 198551: pelitic gneiss, Donnelly River; Geochronology Record 1283: Geological Survey of Western Australia, 6p.

Outhwaite, MD 2018, Metamorphosed Mesoarchean Cu–Mo–Ag mineralization: evidence from the Calingiri deposits, southwest Yilgarn Craton: Geological Survey of Western Australia, Report 183, 208p.

Pisarevsky, SA, Waele, BD, Jones, S, Söderlund, U and Ernst, RE 2015, Paleomagnetism and U–Pb age of the 2.4 Ga Erayinia mafic dykes in the south-western Yilgarn, Western Australia: Paleogeographic and geodynamic implications: Precambrian Research, v. 259, p. 222–231, doi:10.1016/j.precamres.2014.05.023.

Sircombe, KN, Cassidy, KFC, Champion, DC and Tripp, G 2007, Compilation of SHRIMP U–Pb geochronological data, Yilgarn Craton, Western Australia, 2004–2006: Geoscience Australia, Record 2007/01, 182p.

Smithies, RH, Lu, Y, Lowrey, J, Ivanic, T, Champion, DC and Wilde, SA 2021a, Variations in granite geochemistry in the southwest Yilgarn. Geological Survey of Western Australia, digital data layer.

Smithies, RH, Lu, Y and Champion, DC 2021b, New geochemical and geochronological constraints on the magmatic evolution of Boddington, southwest Yilgarn: Geological Survey of Western Australia, digital data layer.

Stark, JC, Wilde, SA, Söderlund, U, Li, Z-X, Rasmussen, B and Zi, J-W 2018, First evidence of Archean mafic dykes at 2.62 Ga in the Yilgarn Craton, Western Australia: Links to cratonisation and the Zimbabwe Craton: Precambrian Research, v. 317, p. 1–13.

Stark, JC, Wang, X-C, Denyszyn, SW, Li, Z-X, Rasmussen, B, Zi, J-W, Sheppard, S and Liu, Y 2019, Newly identified 1.89 Ga mafic dyke swarm in the Archean Yilgarn Craton, Western Australia suggests a connection with India: Precambrian Research, v. 329, p. 156–169, 14p., doi:10.1016/j.precamres.2017.12.036.

Stark, JC, Wang, X-C, Li, Z-X, Denyszyn, SW, Rasmussen, B and Zi, J-W 2018, 1.39 Ga mafic dyke swarm in southwestern Yilgarn Craton marks Nuna to Rodinia transition in the West Australian Craton: Precambrian Research, v. 316, p. 291–304, 14p., doi:10.1016/j.precamres.2018.08.014.

Wilde, SA, Middleton, MF and Evans, BJ 1996, Terrane accretion in the southwestern Yilgarn Craton: Evidence from a deep seismic crustal profile: Precambrian Research, v. 78, p. 179–196.

Wingate, MTD 2007, Proterozoic mafic dykes in the Yilgarn Craton, *in* Proceedings of Geoconferences (WA) Inc. Kalgoorlie '07 Conference, 25–27 September 2007, Kalgoorlie, Western Australia *edited by* FP Bierlein and CM Knox-Robinson: Geoscience Australia, Record 2007/14, p. 80–84.

Wingate, MTD 2017, Mafic dyke swarms and large igneous provinces in Western Australia get a digital makeover, *in* GSWA 2017 extended abstracts: promoting the prospectivity of Western Australia: Geological Survey of Western Australia, Record 2017/2, p. 4–8.

Zibra, I, Clos, F, Weinberg, RF and Peternell, M 2017, The c. 2730 Ma onset of the Neoarchean Yilgarn Orogeny: Tectonics, v. 36, no. 9, p. 1787–1813, doi:10.1002/2017TC004562.

Zibra, I, 2021, Lithostructural map of the Chittering Metamorphic Belt. Geological Survey of Western Australia, digital data layer.

Recommended reference

Quentin de Gromard, R, Ivanic, TJ and Zibra, I 2021, Pre-Mesozoic interpreted bedrock geology of the southwest Yilgarn: Geological Survey of Western Australia, digital data layers.